Rearrangement and Fragmentation Processes on the Potential Energy Surfaces of H_2CS and H_2CS^+

Susan A. Pope,† Ian H. Hillier,† and Martyn F. Guest*

Contribution from the Department of Chemistry, University of Manchester, Manchester M13 9PL, United Kingdom, and Computational Science Group, SERC Daresbury Laboratory, Daresbury, Warrington WA4 4AD, United Kingdom. *Received May 14, 1984*

Abstract: Stationary points on the singlet and triplet surfaces of thioformaldehyde, H_2CS, and on the doublet potential energy surface of the thioformaldehyde cation, H_2CS^+, have been examined by ab initio molecular orbital theory. Equilibrium and transition state geometries have been located using split-valence, triple-ζ valence, and triple-ζ valence plus polarization basis sets, with improved relative energies obtained by means of extensive multireference configuration interaction calculations. Barriers for the dissociation of thioformaldehyde to H_2 + CS and for isomerization to thiohydroxycarbene, HCSH, on the S_0 surface are found to be 89.0 and 79.2 kcal/mol, respectively. An estimate of 85.2 kcal/mol is given for the dissociation to radical products, H + HCS. All three processes are calculated to lie significantly above the origin of singlet absorption, accounting for the failure to observe photodissociation as an important decay process for the $^1A_2$ state of H_2CS. The magnitude of the barrier to dissociation to radical products on the T_1 surface is found to be sensitive to the level of treatment. The energy required for rearrangement of H_2CS (T_1) to thiohydroxycarbene (T_1) is calculated to be 45.7 kcal/mol, with the ^3A HCSH excited state lying some 15.4 kcal/mol above the $^1A'$ state of the trans configuration. $CH_2S^+(^2B_2)$ is predicted to be more stable than *trans*-$HCSH^+$ ($^2A'$) by 30.2 kcal/mol, with a barrier of 55.4 kcal/mol computed for the rearrangement to the less stable isomer. Calculations on the thioformyl radical and thioformyl cation suggest that HCS ($^2A'$) is some 40 kcal/mol more stable than CSH ($^2A'$), while HCS^+ ($^1\Sigma^+$) is more stable than HSC^+ ($^1A'$) by 74.2 kcal/mol. A significant barrier to the 1,2 hydrogen shift isomerization is predicted in the neutral isomer, while that in the cation is predicted to occur without activation energy.

1. Introduction

Thioformaldehyde, H_2CS, has received serious attention only in the last decade, in spite of its obvious role as a prototype system for the thiocarbonyl functional group, >C=S, a moiety of great importance in the chemistry of sulfur-containing organic compounds.[1,2] In contrast, the oxy analogue, formaldehyde (H_2CO), has taken a central place in fundamental molecular photochemistry and photophysics for it is amenable to both detailed and well-defined spectroscopic[3-10] and theoretical studies[11-23] and can behave as a prototype for the photochemistry and photophysics of larger molecules. The overall process is apparently simple, formaldehyde adsorbing light to attain the S_1 state which then dissociates into either molecular (eq 1) or radical products (eq 2). The detailed

$$H_2CO(S_0) \longrightarrow H_2CO(S_1) \longrightarrow \begin{cases} H_2 + CO & (1) \\ H + HCO & (2) \end{cases}$$

mechanism of the photochemistry of formaldehyde remains, however, a tantalizing problem. A large number of associated phenomena have been revealed experimentally, with the exact role of hydroxycarbene, HCOH, a topic of continuing debate.[19,20] A brief outline of the available data on the fragmentation of formaldehyde pertinent to the present study is presented in the following section.

Although the spectroscopy of thioformaldehyde has been the subject of increasing experimental[24-44] and theoretical[33,45-54] interest in recent years, the progression to its photophysics and photochemistry has been little studied.[55,56] It has been suggested[42] that photodissociation may not be an important decay process for the $^1A_2(S_1)$ state of H_2CS, based on the occurrence of strong emission from highly excited vibrational levels ($A^1A_2 \rightarrow X^1A_1$) in both laser fluorescence excitation spectra[42] and laser optoacoustic detection spectra.[36] This is in marked contrast to formaldehyde[57] where dissociative processes become increasingly dominant higher up the potential well, resulting in a termination of intensity of the fluorescence excitation spectra. This effect has been attributed[42] to the lower excitation energy of the $^1A_2$ state in the sulfur molecule (H_2CS, 46.8 kcal/mol;[35] H_2CO, 80.6

† University of Manchester.
* Address correspondence to this author at SERC Daresbury Laboratory.

(1) Berthier, G.; Serre, J. In "The Chemistry of the Carbonyl Group"; Patai, S., Ed.; Interscience: London, 1966; p 1.
(2) Kutzelnigg, W. *Pure Appl. Chem.* **1977**, *49*, 981.
(3) Luntz, A. C. *J. Chem. Phys.* **1978**, *69*, 3436.
(4) Sodeau, J. R.; Lee, E. K. C. *Chem. Phys. Lett.* **1978**, *57*, 71.
(5) Selzle, H. L.; Schlag, E. W. *Chem. Phys.* **1979**, *43*, 111.
(6) Avouris, P.; Gelbart, W. M.; El-Sayed, M. A. *Chem. Rev.* **1977**, *77*, 793.
(7) Weisshaar, J. C.; Moore, C. B. *J. Chem. Phys.* **1979**, *70*, 5135; **1980**, *72*, 2875.
(8) Gelbart, W. M.; Elert, M. L.; Heller, D. F. *Chem. Rev.* **1980**, *80*, 403.
(9) Moore, C. B.; Weisshaar, J. C. *Annu. Rev. Phys. Chem.* **1983**, *34*, 525.
(10) Diem, M.; Lee, E. K. C. *Chem. Phys.* **1979**, *41*, 373.
(11) Heller, D. F.; Elert, M. L.; Gelbart, M. W. *J. Chem. Phys.* **1978**, *69*, 4061.
(12) Lucchesse, R. R.; Schaefer, H. F. *J. Am. Chem. Soc.* **1978**, *100*, 298.
(13) Kemper, M. J. H.; van Dijk, J. M. F.; Buck, H. M. *J. Am. Chem. Soc.* **1978**, *100*, 7841; *J. Chem. Phys.* **1979**, *70*, 2854.
(14) Pople, J. A.; Krishnan, H. B.; Schlegel, R.; Binkley, J. S. *Int. J. Quantum Chem.* **1978**, *14*, 545.
(15) Goddard, J. D.; Schaefer, H. F. *J. Chem. Phys.* **1979**, *70*, 5117.
(16) Miller, W. H. *J. Am. Chem. Soc.* **1979**, *101*, 6810.
(17) Carter, S.; Mills, I. M.; Murrell, J. N. *Mol. Phys.* **1980**, *39*, 455.
(18) Harding, L. B.; Schlegel, H. B.; Krishnan, R.; Pople, J. A. *J. Phys. Chem.* **1980**, *84*, 3394.
(19) Kemper, M. J. H.; Hoeks, C. H.; Buck, H. M. *J. Chem. Phys.* **1981**, *74*, 5744.
(20) Goddard, J. D.; Yamaguchi, Y.; Schaefer, H. F. *J. Chem. Phys.* **1981**, *75*, 3459.
(21) Adams, G. F.; Bent, G. D.; Bartlett, R. J.; Purvis, G. D. *J. Chem. Phys.* **1981**, *75*, 834.
(22) Frisch, M. J.; Krishnan, R.; Pople, J. A. *J. Phys. Chem.* **1981**, *85*, 1467.
(23) Dupuis, M.; Lester, W. A.; Lengsfield, B. H., III; Liu, B. *J. Chem. Phys.* **1983**, *79*, 6167.
(24) Jones, A.; Lossing, F. P. *J. Phys. Chem.* **1967**, *71*, 4111.
(25) Callear, A. B.; Connor, J.; Dickson, D. R. *Nature (London)* **1969**, *221*, 1238.
(26) Johnson, D. R.; Powell, F. X. *Science* **1970**, *169*, 679.
(27) Johnson, D. R.; Powell, F. X.; Kirchhoff, W. R. *J. Mol. Spectrosc.* **1971**, *39*, 136.
(28) Beers, Y.; Klein, G. P.; Kirchhoff, W. H. *J. Mol. Spectrosc.* **1972**, *44*, 479.
(29) Johns, J. W. C.; Olson, W. B. *J. Mol. Spectrosc.* **1971**, *39*, 479.
(30) Turner, P. H.; Halonen, L.; Mills, I. M. *J. Mol. Spectrosc.* **1981**, *88*, 402.
(31) Rock, S. L.; Flygare, W. H. *J. Chem. Phys.* **1972**, *56*, 4723.
(32) Kroto, H. W.; Suffolk, R. J. *Chem. Phys. Lett.* **1972**, *15*, 545.
(33) Solouki, B.; Rosmus, P.; Bock, H. *J. Am. Chem. Soc.* **1976**, *98*, 6054.

0002-7863/85/1507-3789$01.50/0

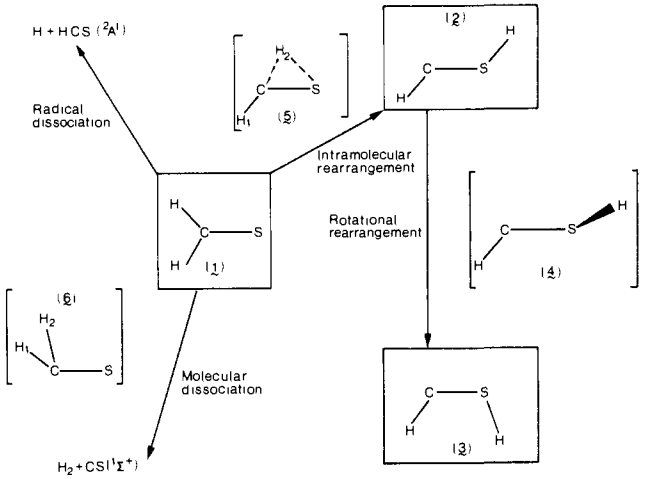

Figure 1. Rearrangement and dissociation processes on the H_2CS S_0 potential energy surface. Transition structures are shown in square brackets.

kcal/mol[58]). In contrast the photochemistry of the dichloro species, thiophosgene, Cl_2CS,[59] is found to resemble that of formaldehyde itself, in that the $^1A_2$ states of both molecules undergo fluorescence and predissociation. The mode of predissociation is apparently different, however, since only radical dissociation of thiophosgene is observed (i.e., $Cl_2CS \rightarrow Cl + SCCl$) from both the ground and first excited singlet states.[59]

Recently a number of experimental and theoretical studies have provided evidence as to the structures and stabilities of the possible isomers of protonated thioformaldehyde, CH_2SH^+.[60-63] In an extensive study of the photoionization mass spectrometry of CH_3SH, CD_3SH, and CH_3SD, indirect evidence has been provided

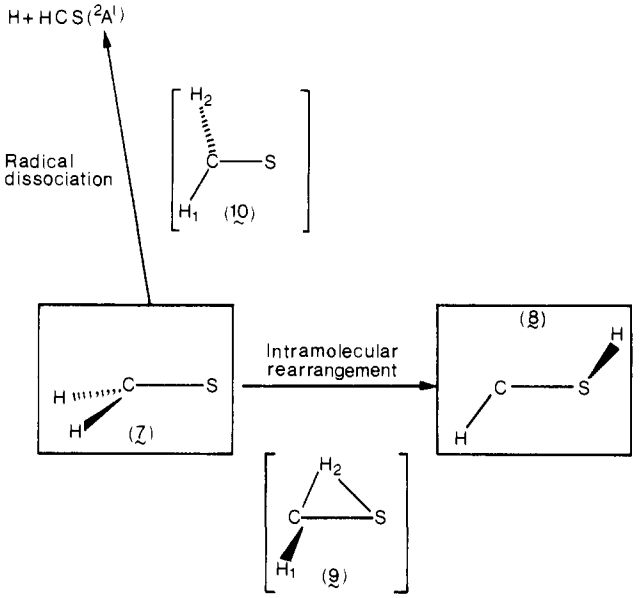

Figure 2. Rearrangement and dissociation processes on the H_2CS T_1 potential energy surface. Transition structures are shown in square brackets.

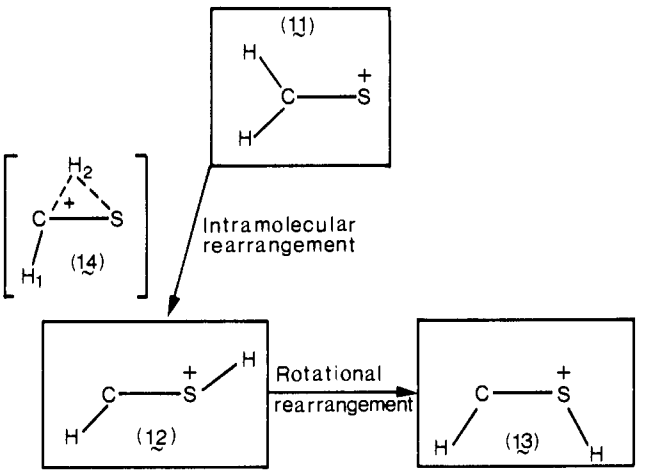

Figure 3. Rearrangement processes on the H_2CS^+ ground-state potential energy surface. The transition structure is shown in square brackets.

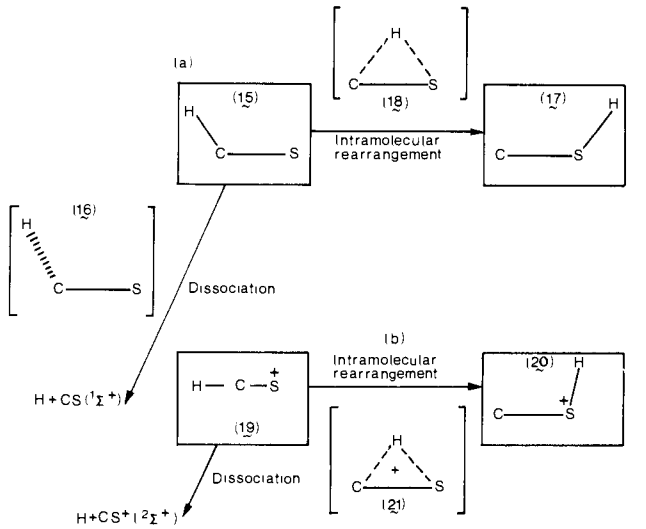

Figure 4. Rearrangement and dissociation processes on the HCS and HCS^+ potential energy surfaces. Transition structures are shown in square brackets.

(34) Fabricant, B.; Kreiger, D.; Muenter, J. S. *J. Chem. Phys.* **1977**, *67*, 1576.
(35) Judge, R. H.; King, C. W. *Can. J. Phys.* **1975**, *53*, 1927.
(36) Dixon, R. N.; Haner, D. A.; Webster, C. R. *Chem. Phys.* **1977**, *22*, 199.
(37) Judge, R. H.; King, C. W. *J. Mol. Spectrosc.* **1979**, *74*, 175; **1979**, *78*, 51.
(38) Dixon, R. N.; Webster, C. R. *J. Mol. Spectrosc.* **1978**, *70*, 314.
(39) Jensen, P.; Bunker, P. R. *J. Mol. Spectrosc.* **1982**, *95*, 92.
(40) Judge, R. H.; Moule, D. C.; King, G. W. *J. Mol. Spectrosc.* **1980**, *81*, 37.
(41) Ramsay, D. A. *J. Photochem.* **1981**, *17*, 505.
(42) Clouthier, D. J.; Kerr, C. M. L.; Ramsay, D. A. *Chem. Phys.* **1981**, *56*, 73.
(43) Jacox, M. E.; Milligan, D. E. *J. Mol. Spectrosc.* **1975**, *58*, 142.
(44) Judge, R. H.; Drury-Lessard, C. R.; Moule, D. C. *Chem. Phys. Lett.* **1978**, *53*, 82.
(45) Fabian, J.; Melhorn, A. *Z. Chem.* **1967**, *7*, 192; **1969**, *9*, 271.
(46) Baird, N. C.; Swenson, J. R. *J. Phys. Chem.* **1973**, *77*, 277.
(47) Bruna, P. J.; Peyerimhoff, S. D.; Buenker, R. J.; Rosmus, P. *Chem. Phys.* **1974**, *3*, 35.
(48) Kapur, A.; Steer, R. P.; Mezey, P. G. *J. Chem. Phys.* **1979**, *70*, 745.
(49) Jaquet, R.; Kutzelnigg, W.; Staemmler, V. *Theor. Chim. Acta* **1980**, *54*, 205.
(50) Whiteside, R. A.; Frisch, M. J.; Binkley, J. S.; DeFrees, D. J.; Schlegel, H. B.; Raghavachari, R.; Pople, J. A. Carnegie Mellon Quantum Chemistry Archive, July 1981.
(51) von Niessen, W.; Cederbaum, L. S.; Domcke, W.; Diercksen, G. H. F. *J. Chem. Phys.* **1977**, *66*, 4893.
(52) Goddard, J. D. *Can. J. Chem.* **1981**, *59*, 3200.
(53) Goddard, J. D.; Clouthier, D. J. *J. Chem. Phys.* **1982**, *76*, 5039.
(54) Burton, P. G.; Peyerimhoff, S. D.; Buenker, R. J. *Chem. Phys.* **1982**, *73*, 83.
(55) Steer, R. P.; Knight, A. R.; Clouthier, D. J.; Moule, D. C. *J. Photochem.* **1978**, *9*, 157.
(56) Clouthier, D. J.; Hackett, P. A.; Knight, A. R.; Steer, R. P. *J. Photochem.* **1981**, *17*, 319.
(57) Lee, E. K. C. *Acc. Chem. Res.* **1977**, *10*, 319.
(58) Horowitz, A.; Calvert, J. G. *Int. J. Chem. Kinet.* **1978**, *10*, 713.
(59) Okabe, H. *J. Chem. Phys.* **1977**, *66*, 2058.

as to the structure and stabilities of the thioformaldehyde cation, H_2CS^+, and the isomeric thiohydroxycarbene cation, $HCSH^+$, and of the thioformyl cation, HCS^+, and the isomer HSC^+.[60]

It is the purpose of the present work to explore theoretically those features of the potential energy surfaces of thioformaldehyde and the thioformaldehyde cation deemed to be of potential significance in leading to an understanding of the dissociation and fragmentation dynamics of both neutral molecule and cation. These features, qualitatively sketched in Figures 1 to 4, may be summarized as follows:

(a) the structure and relative energetics of the ground state ($^1A_1$, S_0, **1**), the first excited triplet state ($^3A_2$, T_1, ($n \rightarrow \pi^*$)), and first excited singlet state ($^1A_2$, S_1, ($n \rightarrow \pi^*$)) of thioformaldehyde;

(b) the structures and relative energetics of the lowest singlet states of *trans*-thiohydroxycarbene (*trans*-HCSH, **2**) and *cis*-thiohydroxycarbene (*cis*-HCSH, **3**), the transition state (**4**) between the rotamers **2** and **3**, and the transition state (**5**) for the H_2CS (S_0) $\rightarrow$ *trans*-HCSH (S_0) rearrangement;

(c) the transition state (**6**) for molecular dissociation of H_2CS (**1**) on the S_0 potential energy surface, and the energetics of the radical dissociation to atomic hydrogen and the thioformyl radical HCS;

(d) the structure and relative energetics of the lowest triplet state of thiohydroxycarbene (T_1, **8**), and the transition state (**9**) for the rearrangement of H_2CS (T_1) to HCSH (T_1, Figure 2); the radical dissociation of H_2CS (T_1) to H and HCS, and the possible radical dissociation transition state (**10**);

(e) features of the ground-state potential surface of the thioformaldehyde cation, H_2CS^+ ($^2B_2$, **11**), including the transition state (**14**) for the intramolecular rearrangement to the *trans*-$HCSH^+$ ion (**12**), and the relative stability of isomeric *cis*-$HCSH^+$ (**13**) (Figure 3);

(f) features of the ground-state potential energy surface of the thioformyl radical and thioformyl cation (Figure 4); the equilibrium structure of the neutral isomers HCS (**15**) and CSH (**17**), the transition states for the radical dissociation process HCS $\rightarrow$ H + CS (**16**), and the intramolecular rearrangement CSH $\rightarrow$ HCS (**18**); the equilibrium structures of the HCS^+ cation (**19**) and CSH^+ isomer (**20**) and the transition state (**21**) for the isomerization $CSH^+ \rightarrow HCS^+$.

Previous experimental and theoretical studies of thioformaldehyde are reviewed in section 3, while the computational details, technical aspects, and results of the present calculations are summarized in section 4, and discussed in section 5. Various aspects of the dissociation and rearrangement processes on the S_0 potential energy surface of H_2CS are presented in section 5.1. In section 5.2 the results of calculations on the T_1 surface are given, while section 5.3 reviews the results for the potential surface of the thioformaldehyde cation. The potential energy surfaces of the thioformyl radical, HCS, and the thioformyl cation are discussed in sections 5.4 and 5.5, respectively. The findings of the present study are summarized in section 6.

2. Photochemistry of Formaldehyde

The experimentally observed phenomena in formaldehyde photochemistry[64-71] are so numerous and diverse that it is unlikely that one simple mechanism exists. It is generally agreed[58] that the molecular process (eq 1) dominates for energies near the S_1 origin at 80.6 kcal/mol, while the importance of the radical process (eq 2) increases with increasing excitation energy. Both processes are symmetry allowed. Substantial activation barriers on the S_1 and T_1 surfaces[69] suggest that dissociation to ground-state radicals takes place on the S_0 surface, since photochemical dissociation is found experimentally[66,68] to occur at energies just below the thermochemical threshold. The exact nature of the long-lived intermediate state between S_1 and the molecular dissociation products[70] remains unclear,[71] and it has been suggested that quantum mechanical tunnelling might be significant in formaldehyde photochemistry.[16]

The ground-state potential surface of H_2CO has been the subject of numerous ab initio molecular orbital calculations,[12-23] culminating in the fourth-order Møller–Plesset studies of Frisch et al.[22] and MCSCF+CI calculations of Dupuis et al.[23] Computed activation barriers for hydrogen elimination of 79.6 and (80.9 ± 2.5) kcal/mol, respectively, represent values slightly below the origin of the formaldehyde excited singlet state, suggesting, in contrast to earlier calculations,[15,18,20,21] that some photochemical dissociation to H_2 + CO takes place without a tunnelling mechanism.

3. Experimental and Theoretical Background

A number of spectroscopic investigations of thioformaldehyde have been conducted following the initial mass spectrometric[24] and UV adsorption[25] studies. The ground-state electronic configuration of H_2CS is $^1A_1$ (. . .$5a_1^2 6a_1^2 2b_2^2 7a_1^2 2b_1^2(\pi) 3b_2^2(n)$). The molecular constants in the ground state have been determined by a variety of methods, including microwave,[26-28] infrared,[29,30] and rotational Zeeman spectroscopy,[31] where a large molecular g value suggested[54] that the excited $n \rightarrow \pi^*$ states should be lower for H_2CS than H_2CO. A vertical ionization potential of 9.34 eV was obtained using photoelectron spectroscopy (PES),[32] in reasonable agreement with the value of 9.44 eV determined originally.[24] An estimate of 9.30 eV has been given for the adiabatic value.[59] PES was also used to identify H_2CS prepared by a gas-phase synthesis,[33] as opposed to earlier photolysis or pyrolysis methods (note that H_2CS is highly reactive and will readily trimerize to *s*-trithiane). Confirmation of the microwave value of 1.647 D for the ground-state dipole moment[27] was provided by molecular beam electric resonance measurements[34] (1.6491 D).

Values of 1.80 and 2.03 eV have been obtained for the (0–0) transitions to the dipole-forbidden ($n \rightarrow \pi^*$) $^3A_2$ and $^1A_2$ states,[35] the latter value having been confirmed by optoacoustic spectroscopy.[36] A dipole moment of 0.79 D[38] has been determined for the $^1A_2$ state, which was found to possess a slightly nonplanar geometry.[37] Calculations using the semirigid invertor Hamiltonian[39] suggest, however, a planar geometry for this state. An analysis of the $a^3A_2 \leftarrow X^1A_1$ absorption band has yielded an r_0 structure for the lowest triplet state.[40]

Previous theoretical studies of thioformaldehyde have concentrated in the main on calculations of the photoelectron[33,51] and UV absorption spectra.[45-47,54] As noted by Burton et al.,[54] "Quantitative accounting of the structural features of even the ground state of H_2CS has not yet become impressive, even when extensive CI calculations have been undertaken, presumably because of limitations inherent in the rather small basis sets that have been used." A summary of the results of previous theoretical studies on the ground state is given in Table I. The excellent agreement between the CEPA geometry[49] and experiment is worthy of note, although the rather small basis set employed in those calculations suggests that the agreement is perhaps "somewhat fortuitous".[49]

The outer valence ionization potentials have been calculated by both CI[33] and a many-body Greens function method,[51] the calculated values showing satisfactory agreement with experiment[33]

(60) Kutina, R. E.; Edwards, A. K.; Goodman, G. L.; Berkowitz, J. *J. Chem. Phys.* **1982**, *77*, 5508.
(61) Dill, J. D.; McLafferty, F. W. *J. Am. Chem. Soc.* **1979**, *101*, 6526.
(62) Roy, M.; McMahon, T. B. *Org. Mass Spectrom.* **1982**, *17*, 392.
(63) Pope, S. A.; Hillier, I. H.; Guest, M. F. *Chem. Phys. Lett.* **1984**, *104*, 191.
(64) Norrish, R. G. W.; Kirkbride, F. W. *J. Chem. Soc.* **1932**, 1518. Norrish, R. G. W. *Trans. Faraday Soc.* **1934**, *30*, 103.
(65) Benson, S. W. "Thermochemical Kinetics", 2nd ed.; Wiley-Interscience: New York, 1976.
(66) Clark, J. H.; Moore, C. B.; Nogar, N. S. *J. Chem. Phys.* **1978**, *68*, 1264.
(67) Herzberg, G. "Electronic Spectra of Polyatomic Molecules"; Van Nostrand: Princeton, 1966; pp 589, 612.
(68) Reilly, J. P.; Clark, J. H.; Moore, C. B.; Pimentel, G. C. *J. Chem. Phys.* **1978**, *69*, 4381.
(69) Hayes, D. M.; Morokuma, K. *Chem. Phys. Lett.* **1972**, *12*, 539.
(70) Houston, P. L.; Moore, C. B. *J. Chem. Phys.* **1976**, *65*, 757.
(71) Weisshaar, J. C.; Baronovski, A. P.; Cabello, A.; Moore, C. B. *J. Chem. Phys.* **1978**, *69*, 4720.

Table I. Total Energies (Hartree) and Ground-State Equilibrium Geometry[a] of Thioformaldehyde (X^1A_1) from Previous Theoretical Treatments

level of theory	total energy	r(C-S)	r(C-H)	HCH	ref
HF/STO-3G//STO-3G[b]	-431.671 37	1.574	1.090	112.0	48, 52
HF/STO-3G+d//STO-3G+d	-431.708 75	1.551	1.093	111.7	52
HF/3-21G//3-21G	-434.336 25	1.638	1.073	116.4	50, 52
HF/4-31G//4-31G	-435.991 88	1.629	1.073	115.5	52
HF/DZ//DZ	-436.458 84	1.637	1.075	115.9	52
HF/DZ+P	-436.378 07	(1.611)	(1.093)	(116.9)	51
HF/DZ+P//DZ+P	-436.401 1	1.594	1.084	115.2	49
HF/DZ+P//DZ+P	-436.511 63	1.601	1.080	115.7	52
HF/77 g.t.o.s	-436.542 69	(1.611)	(1.093)	(116.8)	54
HF/96 g.t.f.s	-436.533 20				33
CEPA2/DZP//CEPA2/DZP	-436.696 4	1.613	1.095	115.3	49
PNOCI/DZP//PNOCI/DZP	-436.657 5	1.602	1.092	115.1	49
CEPA2/96 g.t.f.s	-436.834 9				33
MRDCI/77 g.t.o.s.	-436.807 4	(1.611)	(1.093)	(116.8)	54
MRDCI/77 g.t.o.s + full CI estimate[c]	-436.865 6	(1.611)	(1.093)	(116.8)	54
expt. r_0		1.6108	1.0925	116.8	27

[a] All distances in Å: values in parentheses are assumed rather than optimized. [b] Indicates a HF/STO-3G calculation at a geometry optimized at the HF/STO-3G level. [c] Applying a fifth-order size consistency correction.[87]

for the first three IPs, with a maximum deviation of 0.26 eV. The vibrational structure in the PES has also been calculated,[51] with good agreement obtained for the vibrational structure of the first two bands.

Calculated vertical transition energies to the $^3A_2$ and $^1A_2$ states have been determined semiempirically[45] (1.52 and 1.88 eV, respectively), and by ab initio SCF[46] (1.68 and 2.36 eV) and SCF/CI techniques[47] (1.84 and 2.17 eV), values to be compared with the experimental 0–0 values of 1.80 and 2.03 eV, respectively. The excellent agreement given by the SCF/CI study is due primarily to the rather simple valence character of these states, and to the small geometry change associated with ($n \rightarrow \pi^*$) excitation. In the same study two allowed transitions to Rydberg states were predicted to lie in the UV at vertical transition energies of 5.83 eV ($^1B_2$, $n \rightarrow s_R$) and at 6.62 eV ($^1A_1$, $n \rightarrow p_{xR}$). These values were subsequently confirmed experimentally,[44] with 0–0 transition energies of 5.83 and 6.59 eV obtained.

Although these theoretical studies were highly successful in handling the lowest intravalence and valence-Rydberg states (based largely on experience gained from earlier studies on H_2CO[72]), problems were encountered in describing the spectroscopic $\tilde{B}$ state corresponding to the $^1(\pi \rightarrow \pi^*)$ transition. A significant discrepancy is found between the theoretical vertical energy separation of 7.92 eV and experiment, where a value of 5.72 eV has been determined, with a maximum in absorption in the 6.0–6.5 eV range. This discrepancy is perhaps not surprising, in view of similar difficulties encountered when handling the corresponding transition in H_2CO.[73] Attempts to rationalize the discrepancy have been undertaken in the form of extensive multireference double excitation CI (MRD–CI) calculations[54] employing a large atomic orbital basis of 77 functions, including polarization, bond, and Rydberg functions. This study revealed not only the importance of the anticipated large geometry changes between the $\tilde{X}$ and $\tilde{B}$ states in accounting for the experimental 0–0 transition energy, but suggested that an approach close to the full CI limit was required, with due account given to the important mixing of the $^1(\pi \rightarrow \pi^*)$ valence and $^1(\pi \rightarrow d_{\pi R})$ Rydberg configurations.

Ab initio calculations on thiohydroxycarbene appear limited to minimal (STO-3G) and split valence (3-21G) basis set SCF studies,[50] providing estimates of 46.7 and 60.6 kcal/mol respectively for the energy separation between H_2CS (S_0) and *trans*-HCSH (S_0). We are unaware of any previous studies of the H_2CS (S_0) → *trans*-HCSH (S_0) rearrangement, or the stability of the cis isomer. Furthermore, no previous attention appears to have been given to either the radical or molecular dissociation of thioformaldehyde.

4. Computational Details and Results

Geometric structures at the minima and saddle points on the potential energy surfaces under consideration were located by spin-restricted Hartree–Fock calculations using basis sets of increasing size, in conjunction with analytical gradient methods. The basis sets used in obtaining optimized geometrical structures were the split-valence 3-21G set,[74] a triple-ζ (TZ) valence basis[75,76] designated C(10s6p/5s3p), S(12s9p/6s5p), and H(5s/3s), and the triple-zeta plus d-polarization set (TZ+d). In the latter basis, sets of six d functions were centered on sulfur (ζ = 0.542) and carbon (ζ = 0.72).[77] Subsequent to optimization of the TZ+d stationary point geometries, single calculations were conducted at these points with highly correlated wave functions. Single reference state and multireference state CI calculations (hereafter referred to as SDCI and MRDCI, respectively) were performed including all single and double excitations of the valence electrons using the direct-CI method.[78] CI calculations conducted at the HF/TZ+d geometries employed a TZ+2d1p basis comprising the TZ basis augmented by two sets of polarization functions on both sulfur (ζ = 0.95, 0.32) and carbon (ζ = 1.0, 0.30)[79] and a single set of 2p functions on hydrogen (ζ = 1.00).[77] In the MRDCI calculations all configurations having coefficients greater than 0.04 were included in the reference set, yielding up to 298 000 configurations; details of both CI treatments are given in Table II, with specifications of the size of the secular problem and magnitude of the leading terms in the CI expansion ($\Sigma_{ref} c_{ref}^2$) for each of the species under consideration.

Estimates of the importance of higher (than double) excitations, specifically unlinked clusters, were obtained from the SDCI calculations using the modification of Davidson's correction[80] due to Pople et al.[81] (hereafter referred to as the quadruples correction[80] (QC) or PSK correction after Pople et al.); specifically the correction is

$$(1 - 2/n)(1 - c_0^2)\Delta E_{CISD}$$

where c_0 is the coefficient of the Hartree–Fock configuration in

(72) Peyerimhoff, S. D.; Buenker, R. J.; Kammer, W. E.; Hsu, H. *Chem. Phys. Lett.* **1971**, *8*, 129.
(73) Peyerimhoff, S. D.; Buenker, R. J. *Adv. Quantum Chem.* **1975**, *9*, 69.
(74) Binkley, J. S.; Pople, J. A.; Hehre, W. J. *J. Am. Chem. Soc.* **1980**, *102*, 939. Gordon, M. S.; Binkley, J. S.; Pople, J. A.; Pietro, W. J.; Hehre, W. J. *Ibid.* **1982**, *104*, 2797.
(75) Dunning, T. H., Jr. *J. Chem. Phys.* **1971**, *55*, 716.
(76) McLean, A. D.; Chandler, G. S. *J. Chem. Phys.* **1980**, *72*, 5639.
(77) Ahlrichs, R.; Taylor, P. R. *J. Chim. Phys.* **1981**, *78*, 315.
(78) Siegbahn, P. E. M. *J. Chem. Phys.* **1980**, *72*, 1647. Saunders, V. R.; van Lenthe, J. H. *Mol. Phys.* **1983**, *48*, 923.
(79) Ahlrichs, R.; Driessler, F.; Lischka, H.; Staemmler, V.; Kutzelnigg, W. *J. Chem. Phys.* **1975**, *62*, 1235. Ahlrichs, R.; Lischka, H.; Zurawski, B.; Kutzelnigg, W. *Ibid.* **1975**, *63*, 4685.
(80) Langhoff, S. R.; Davidson, E. R. *Int. J. Quantum Chem.* **1974**, *8*, 61. Davidson, E. R.; Silver, D. W. *Chem. Phys. Lett.* **1978**, *52*, 403.
(81) Pople, J. A.; Seeger, R.; Krishnan, R. *Int. J. Quantum Chem.* **1977**, *S11*, 149.

Table II. Technical Details of the CI/TZ+2d1p//TZ+d Calculations

species	symmetry	electronic state	SDCI/TZ+2d1p//TZ+d secular equation	SDCI/TZ+2d1p//TZ+d $C_0^2 \times 100$	nM^a	MRDCI/TZ+2d1p//TZ+d secular equation	MRDCI/TZ+2d1p//TZ+d $\sum_n c_n^2 \times 100$
H_2CS (**1**)	C_{2v}	$^1A_1$	18320	88.8	3	71468	89.7
trans-HCSH (**2**)	C_s	$^1A'$	35953	88.7	4	163689	88.8
cis-HCSH (**3**)	C_s	$^1A'$	35953	88.7	4	163689	88.8
TS (**2** → **3**) (**4**)	C_1	^1A	65341	88.7	2	205525	88.4
TS (**1** → **2**) (**5**)	C_s	$^1A'$	35953	87.8	3	134843	87.8
TS (**1** → H_2 + CS) (**6**)	C_s	$^1A'$	35953	87.6	3	141573	88.3
H_2CS (**7**)	C_s	$^3A''$	123959	89.3	2	204567	89.4
H_2CS	C_s	$^1A''$	74542	89.4	2	123616	89.5
HCSH (**8**)	C_1	^3A	241095	89.3			
TS (**7** → **8**) (**9**)	C_1	^3A	241095	88.0			
TS (**7** → H + HCS) (**10**)	C_1	^3A	241095	86.9			
H_2CS^+ (**11**)	C_{2v}	$^2B_2$	35412	89.0	3	136948	89.6
H_2CS^+	C_{2v}	$^2B_1$	36827	89.8			
trans-$HCSH^+$ (**12**)	C_s	$^2A'$	69225	88.8	3	269895	89.3
cis-$HCSH^+$ (**13**)	C_s	$^2A'$	69225	88.9	3	269895	89.5
TS (**11** → **12**) (**14**)	C_s	$^2A'$	69225	88.5	3	265318	88.5
HCS (**15**)	C_s	$^2A'$	55781	88.4	4	260097	89.2
TS (**15** → H + CS) (**16**)	C_s	$^2A'$	55781	86.7	4	253093	87.2
CS	$C_{\infty v}$	$^1\Sigma^+$	8724	88.5	4	66263	89.1
CSH (**17**)	C_s	$^2A'$	55781	88.5	4	259469	88.5
TS (**15** → **17**) (**18**)	C_s	$^2A'$	55781	87.8	4	298332	87.7
HCS^+ (**19**)	$C_{\infty v}$	$^1\Sigma^+$	11122	89.0	4	85195	90.4
CSH^+ (**20**)	C_s	$^1A'$	20626	88.1	5	176747	88.4
TS (**19** → **20**) (**21**)	C_s	$^1A'$	20626	88.2	5	175318	88.2
CS^+	$C_{\infty v}$	$^2\Sigma^+$	15490	88.8	5	94296	88.8

[a] Number of reference configurations.

the CI expansion, ΔE_{CISD} the energy lowering due to the singly and doubly excited configurations, and n the number of electrons. Where noted, corresponding estimates were obtained from the MRDCI calculations using the generalized form of Davidson's correction.[82-84] Finally harmonic vibrational frequencies were obtained for stationary points on the HF/3-21G surface, serving to characterize minima and saddle points, and allowing for the determination of zero-point vibrational energies (ZPVE's).

All calculations were carried out on the CRAY-1S computer at the SERC Daresbury Laboratory using the program system GAMESS.[85]

Optimized geometries for stationary points on the H_2CS and H_2CS^+ potential energy hypersurfaces are given in Table III. We subsequently use the notation MRDCI/TZ+2d1p//TZ+d, for example, to indicate a multireference CI calculation with the TZ+2d1p basis set at a geometry optimized at the HF/TZ+d level. Total energies and zero-point vibrational energies of all the minima and saddle points considered in the present study are listed in Table IV. Since vibrational frequencies at the HF/3-21G level are generally overestimated by about 10%,[86] the calculated zero-point energies of Table IV are scaled by 0.9 when used in the evaluation of reaction energies and barrier heights.

5. Discussion

5.1 Dissociation and Rearrangement on the S_0 Potential Energy Surface of H_2CS. The various aspects of the dissociation and rearrangement processes on the S_0 potential energy surface of thioformaldehyde will be discussed under four separate headings: (a) the equilibrium structure of H_2CS (X^1A_1), (b) the rearrangement to thiohydroxycarbene, (c) the molecular dissociation of thioformaldehyde, and finally (d) the radical dissociation of thioformaldehyde. Relative energies at various levels of theory for H_2CS and component systems are summarized in Table V.

A. Equilibrium Structure of H_2CS (X^1A_1). The total energies of thioformaldehyde (**1**) at various levels of calculation are shown in Table IV, while the optimized geometries obtained at the 3-21G, TZ, and TZ+d levels are given in Table III. The HF/TZ+2d1p//TZ+d energy is 7.5×10^{-3} hartree lower than that obtained in the 77 AO basis calculation of Burton et al.[54] Comparison of the optimized geometries with the experimentally determined r_e structure[27] suggests that at the HF/TZ+d level both the C–S and the C–H bonds are slightly too short (by 0.011 and 0.015 Å, respectively), and the HCH angle is slightly too small (by 1.2°). Such errors are consistent with those expected from near-Hartree–Fock-limit SCF geometries.[88] Table VI shows a comparison of the harmonic frequencies predicted at the HF/3-21G level of theory with reported experimental[29,30] and previous theoretical[49,53] estimates. As expected[86] the predicted harmonic frequencies are larger than the corresponding experimental values, the deviations from experiment being due to the neglect of both electron correlation and anharmonicity in the theoretical work. Scaling the 3-21G frequencies by a factor of 0.9 yields values which lie within 85 cm^{-1} of the experimental data. It is perhaps worth noting that the MRDCI/TZ+2d1p//TZ+d energy of −436.85134 hartrees is the lowest variational energy yet calculated for H_2CS (X^1A_1) and may be compared with the best previous value of −436.80741 hartrees.[54] A final CI energy of −436.8753 hartrees is given on applying the generalized PSK correction to the MRDCI result, a value 1.0×10^{-2} hartree lower than the corresponding estimate from ref 54. The computed dipole moment of 1.79 D at the MRDCI/TZ+2d1p//TZ+d level is in somewhat better agreement with the experimental (r_0) value of 1.65 D than a previous MRDCI estimate of 1.87 D.[54]

B. Rearrangement of Thioformaldehyde to Thiohydroxycarbene. The total energies of *trans*-thiohydroxycarbene (**2**), *cis*-thiohydroxycarbene (**3**), the transition state between these rotamers (**4**), and the transition state (**5**) for the H_2CS (S_0) → *trans*-HCSH (S_0) rearrangement are given in Table IV. Optimized geometries for each species are shown in Table III. The MRDCI calculations predict the *trans*-HCSH → H_2CS rearrangement to be exothermic

(82) Hirsch, G.; Bruna, P. J.; Peyerimhoff, S. D.; Buenker, R. J. *Chem. Phys. Lett.* **1977**, *52*, 442.
(83) Butscher, W.; Shih, S.-K.; Buenker, R. J.; Peyerimhoff, S. D. *Chem. Phys. Lett.* **1977**, *52*, 457.
(84) Bruna, P. J.; Buenker, R. J.; Peyerimhoff, S. D. *Chem. Phys. Lett.* **1980**, *72*, 278.
(85) Dupuis, M.; Spangler, D.; Wendoloski, J. J. N.R.C.C. Software Catalog, Vol. 1, Program No. QG01, 1980. Guest, M. F.; Kendrick, J.; Pope, S. A. GAMESS Documentation: Daresbury Laboratory, 1983.
(86) Pople, J. A.; Schlegel, H. B.; Krishnan, R.; Defrees, D. J.; Binkley, J. S.; Frisch, M. J.; Whiteside, R. A.; Hout, R. F.; Hehre, W. J. *Int. J. Quantum Chem.* **1981**, *15*, 269. Pulay, P. In "Modern Theoretical Chemistry"; Schaefer, H. F., Ed.; Plenum Press: New York, 1977; Vol. 4.
(87) Wilson, S.; Silver, D. M. *Theor. Chim. Acta* **1979**, *54*, 83.
(88) Pople, J. A. In "Modern Theoretical Chemistry"; Schaefer, H. F., III, Ed.; Plenum Press: New York, 1977; Vol. 4.

Table III. Optimized Geometrical Parameters[a] for Stationary Points on the H_2CS and H_2CS^+ Potential Energy Hypersurfaces[b]

parameter	3-21G	TZ	TZ+d
1, H_2CS (C_{2v}, X^1A_1)			
r(C-H)	1.073	1.072	1.078
r(C-S)	1.638	1.640	1.600
∠HCS	121.8	121.9	122.2
2, *trans*-HCSH (C_s, $^1A'$)			
r(C-H)	1.095	1.095	1.091
r(C-S)	1.788	1.776	1.675
r(S-H)	1.349	1.359	1.339
∠SCH	103.5	104.4	104.4
∠CSH	99.1	99.2	100.1
3, *cis*-HCSH (C_s, $^1A'$)			
r(C-H)	1.095	1.095	1.086
r(C-S)	1.775	1.768	1.666
r(S-H)	1.363	1.374	1.352
∠SCH	108.6	109.5	110.6
∠CSH	106.8	106.2	106.7
4, HCSH, Rotation Transition Structure (C_1, ^1A)			
r(C-H)	1.099	1.099	1.093
r(C-S)	1.970	1.930	1.837
r(S-H)	1.359	1.369	1.343
∠SCH	101.8	104.0	104.5
∠CSH	93.5	94.1	90.4
$\angle HCSH_2$	88.0	88.6	89.5
5, Transition Structure: $H_2CS \rightarrow$ *trans*-HCSH (C_s, $^1A'$)			
$r(C-H_1)$	1.085	1.085	1.086
$r(C-H_2)$	1.446	1.435	1.379
r(C-S)	1.794	1.782	1.694
$r(S-H_2)$	1.530	1.517	1.474
$\angle SCH_1$	117.2	117.5	116.7
$\angle SCH_2$	55.1	55.1	56.2
6, Transition Structure: $H_2CS \rightarrow H_2 + CS$ (C_s, $^1A'$)			
$r(C-H_1)$	1.176	1.187	1.188
$r(C-H_2)$	1.520	1.500	1.406
r(C-S)	1.630	1.636	1.594
$\angle SCH_1$	145.5	144.7	139.5
$\angle SCH_2$	105.4	104.5	98.8
7, H_2CS (C_s, $^3A''$)			
r(C-H)	1.072	1.070	1.074
r(C-S)	1.807	1.795	1.737
∠HCS	116.6	117.7	117.3
H_2CS (C_s, $^1A''$)			
r(C-H)	1.071	1.070	1.074
r(C-S)	1.827	1.812	1.760
∠HCS	116.7	117.7	117.1
8, HCSH (C_1, ^3A)			
r(C-H)	1.074	1.074	1.075
r(C-S)	1.810	1.803	1.737
r(S-H)	1.355	1.366	1.339
∠HCS	126.5	128.0	128.2
∠CSH	98.6	99.0	98.4
∠HCSH	98.3	97.6	94.2
9, Transition Structure: $H_2CS \rightarrow$ *trans*-HCSH (C_1, ^3A)			
$r(C-H_1)$	1.073	1.072	1.075
$r(C-H_2)$	1.432	1.422	1.393
r(C-S)	1.842	1.826	1.736
$\angle SCH_1$	127.7	129.1	129.0
$\angle SCH_2$	54.0	54.1	54.8
∠HSCH	98.6	99.6	95.0
10, Transition Structure: $H_2CS \rightarrow$ HCS+H (C_1, ^3A)			
$r(C-H_1)$	1.075	1.074	1.078
$r(C-H_2)$	1.787	1.779	1.732
r(C-S)	1.626	1.627	1.580
$\angle H_1CS$	134.7	136.0	133.5
$\angle H_2CS$	105.7	106.8	102.4
11, H_2CS^+ (C_{2v}, $^2B_2$)			
r(C-H)	1.079	1.078	1.081
r(C-S)	1.645	1.649	1.601
∠HCS	120.6	120.8	120.6
H_2CS^+ (C_{2v}, $^2B_1$)			
r(C-H)	1.078	1.078	1.080
r(C-S)	1.822	1.812	1.732
∠HCS	120.5	120.7	120.9
12, *trans*-$HCSH^+$ (C_s, $^2A'$)			
r(C-H)	1.075	1.076	1.078
r(C-S)	1.648	1.652	1.597
r(S-H)	1.362	1.377	1.347
∠SCH	135.4	135.8	134.7
∠CSH	99.5	99.0	97.5
13, *cis*-$HCSH^+$ (C_s, $^2A'$)			
r(C-H)	1.075	1.076	1.077
r(C-S)	1.647	1.652	1.595
r(S-H)	1.365	1.380	1.349
∠SCH	143.0	143.3	140.7
∠CSH	100.6	99.7	98.5
14, Transition Structure: $H_2CS^+ \rightarrow$ *trans*-$HCSH^+$ (C_s, $^2A'$)			
$r(C-H_1)$	1.073	1.075	1.080
$r(C-H_2)$	1.491	1.461	1.407
r(C-S)	1.640	1.638	1.573
$r(S-H_2)$	1.462	1.560	1.498
$\angle SCH_1$	146.2	146.8	146.6
$\angle SCH_2$	60.0	60.1	60.1
15, HCS (C_s, $^2A'$)			
r(C-H)	1.073	1.073	1.077
r(C-S)	1.602	1.604	1.557
∠HCS	135.6	136.7	134.6
16, Transition Structure: HCS → H + CS (C_s, $^2A'$)			
r(C-H)	1.780	1.779	1.739
r(C-S)	1.574	1.574	1.527
∠HCS	116.9	119.4	118.6
17, CSH (C_s, $^2A'$)			
r(C-S)	1.814	1.793	1.679
r(S-H)	1.357	1.367	1.345
∠HSC	100.7	100.9	100.9
18, Transition Structure: HCS → CSH (C_s, $^2A'$)			
r(C-H)	1.459	1.446	1.447
r(C-S)	1.805	1.787	1.678
r(S-H)	1.526	1.510	1.439
∠HCS	54.5	54.4	54.2
19, HCS^+ ($C_{\infty v}$, $^1\Sigma^+$)			
r(C-H)	1.068	1.070	1.073
r(C-S)	1.495	1.492	1.455
20, CSH^+ (C_s, $^1A'$)			
r(C-S)	1.672	1.682	1.607
r(S-H)	1.379	1.393	1.369
∠HSC	99.4	97.2	86.1
21, Transition Structure: $HCS^+ \rightarrow CSH^+$ (C_s, $^1A'$)			
r(C-H)	1.434	1.360	1.281
r(C-S)	1.610	1.610	1.534
r(S-H)	1.696	1.693	1.648
∠HSC	67.4	68.9	71.1
CS ($^1\Sigma^+$)			
r(C-S)	1.564	1.564	1.518
CS^+ ($^2\Sigma^+$)			
r(C-S)	1.508	1.505	1.459
H_2 ($^1\Sigma_g^+$)			
r(H-H)	0.735	0.732	0.732

[a] See Figures 1-4 for atom numbering. [b] All bond lengths in Å, angles in deg.

by 48.7 kcal/mol, to be compared with the value of 47.2 kcal/mol given at the SDCI level. Corresponding values of 47.1 and 47.4 kcal/mol are given on applying the appropriate unlinked cluster correction.

Table IV. Calculated Total Energies and Zero-Point Vibrational Energies[a] for the H_2CS and H_2CS^+ Component Systems

species	sym-metry	electronic state	HF/3-21G //3-21G	HF/TZ //TZ	HF/TZ+2d1p //TZ+d	SDCI/TZ+ 2d1p//TZ+d	MRDCI/TZ+ 2d1p//TZ+d	ZPVE
H_2CS (**1**)	C_{2v}	$^1A_1$	−434.336 24	−436.493 25	−436.550 23	−436.842 71	−436.851 34	16.7
trans-HCSH (**2**)	C_s	$^1A'$	−434.239 70	−436.400 74	−436.482 71	−436.767 51	−436.773 75	13.8
cis-HCSH (**3**)	C_s	$^1A'$	−434.234 25	−436.395 42	−436.479 53	−436.764 26	−436.770 47	13.4
TS (**2** → **3**) (**4**)	C_1	^1A	−434.200 56	−436.360 51	−436.428 40	−436.706 76	−436.708 29	11.7
TS (**1** → **2**) (**5**)	C_s	$^1A'$	−434.161 60	−436.327 09	−436.402 22	−436.702 51	−436.710 37	10.8
TS (**1** → H_2 + CS) (**6**)	C_s	$^1A'$	−434.145 52	−436.305 83	−436.384 43	−436.686 82	−436.695 38	9.8
H_2CS (**7**)	C_s	$^3A''$	−434.309 39	−436.467 31	−436.509 22	−436.783 06	−436.784 67	15.0
H_2CS	C_s	$^1A''$	−434.304 29	−436.462 22	−436.502 52	−436.775 08	−436.776 16	15.1
HCSH (**8**)	C_1	^3A	−434.257 61	−436.417 92	−436.479 89	−436.745 24		13.1
TS (**7** → **8**) (**9**)	C_1	^3A	−434.186 72	−436.351 11	−436.413 96	−436.700 25		10.9
TS (**7** → H + HCS) (**10**)	C_1	^3A	−434.185 46	−436.341 94	−436.399 91	−436.688 27		9.8
H_2CS^+ (**11**)	C_{2v}	$^2B_2$	−434.024 35	−436.183 18	−436.245 87	−436.514 75	−436.524 20	16.2
H_2CS^+	C_{2v}	$^2B_1$	−433.963 21	−436.124 35	−436.177 78	−436.433 29		
trans-$HCSH^+$ (**12**)	C_s	$^2A'$	−433.950 39	−436.113 19	−436.198 56	−436.463 24	−436.472 37	13.9
cis-$HCSH^+$ (**13**)	C_s	$^2A'$	−433.946 14	−436.109 55	−436.196 11	−436.459 77	−436.468 86	13.5
TS (**11** → **12**) (**14**)	C_s	$^2A'$	−433.874 88	−436.041 41	−436.132 53	−436.416 18	−436.426 06	10.8
HCS (**15**)	C_s	$^2A'$	−433.701 56	−435.856 94	−435.917 15	−436.192 06	−436.203 74	7.8
TS (**15** → H + CS) (**16**)	C_s	$^2A'$	−433.608 30	−435.762 61	−435.832 15	−436.110 07	−436.121 94	2.4
CSH (**17**)	C_s	$^2A'$	−433.638 53	−435.798 76	−435.867 95	−436.129 96	−436.136 67	5.9
TS (**15** → **17**) (**18**)	C_s	$^2A'$	−433.568 72	−435.733 49	−435.810 91	−436.091 34	−436.100 66	3.7
HCS^+ (**19**)	$C_{\infty v}$	$^1\Sigma^+$	−433.418 06	−435.573 87	−435.655 60	−435.924 33	−435.941 67	9.6
CSH^+ (**20**)	C_s	$^1A'$	−433.290 94	−435.452 64	−435.546 32	−435.804 70	−435.817 80	5.7
TS (**19** → **20**) (**21**)	C_s	$^1A'$	−433.257 02	−435.424 13	−435.530 88	−435.800 48	−435.815 82	3.7
CS	$C_{\infty v}$	$^1\Sigma^+$	−433.122 93	−435.275 98	−435.347 48	−435.611 08	−435.625 67	1.8
CS^+	$C_{\infty v}$	$^2\Sigma^+$	−432.719 36	−434.873 97	−434.958 34	−435.205 48	−435.224 26	2.0
H_2	$D_{\infty h}$	$^1\Sigma_g^+$	−1.122 96	−1.128 03	−1.132 62	−1.167 39		6.5
H		^2S	−0.496 20	−0.499 81				

[a] Total energies in hartrees; zero-point vibrational energies (ZPVE's) obtained at the HF/3-21G level, in kcal/mol.

Table V. Calculated Relative Energies (kcal/mol) for the H_2CS Component Systems[a]

species	sym-metry	electronic state	HF/TZ //TZ	HF/TZ+2d1p //TZ+d	SDCI/TZ+2d1p //TZ+d	MRDCI/TZ+2d1p //TZ+d	SDCI + ZPVE + QC	MRDCI + ZPVE
H_2CS (**1**)	C_{2v}	$^1A_1$	0.0	0.0	0.0	0.0	0.0	0.0
trans-HCSH (**2**)	C_s	$^1A'$	58.1	42.4	47.2	48.7	44.8	46.1 (44.5)
cis-HCSH (**3**)	C_s	$^1A'$	61.4	44.4	49.2	50.8	46.5	47.8
TS (**2** → **3**) (**4**)	C_1	^1A	83.3	76.5	85.3	89.8	81.4	85.3
TS (**1** → **2**) (**5**)	C_s	$^1A'$	104.3	92.9	88.0	88.5	80.6	83.2 (79.2)
TS (**1** → H_2 + CS) (**6**)	C_s	$^1A'$	117.7	104.1	97.8	97.9	89.2	91.7 (89.0)
H_2CS (**7**)	C_s	$^3A''$	16.3	25.7	37.4	41.8	37.7	40.3 (40.1)
H_2CS	C_s	$^1A''$	19.5	29.9	42.4	47.2	43.1	45.7 (45.7)
HCSH (**8**)	C_1	^3A	47.3	44.1	61.2		60.2	
TS (**7** → **8**) (**9**)	C_1	^3A	89.2	85.5	89.4		83.4	
TS (**7** → H + HCS) (**10**)	C_1	^3A	95.0	94.3	96.9		88.1	
H_2 + CS			56.0	44.0	40.3	36.6	34.6	29.0 (30.6)
H + HCS			85.7	83.7	94.7	92.8	87.5	84.8 (85.2)

[a] Values in parentheses include generalized QC contribution (MRDCI + QC + ZPVE).

Table VI. Harmonic Vibrational Frequencies (cm^{-1}) for H_2CS (X^1A_1), *trans*-HCSH (**2**), and *cis*-HCSH (**3**)

H_2CS								HCSH			
		frequency								frequency[a]	
		exptl		SCF		CEPA					
symmetry	assignment	*b*	*c*	*d*	*e*	*d*	*a*	symmetry	assignment	trans	cis
A_1	C–S stretch	(1150)	(1059)	1134	1053	1113	974	A′	C–S stretch	633	618
	C–H stretch	2971		3200	2937	3215	2975		C–S–H bend	864	844
	H–C–H bend	(1550)	1457	1577	1464	1567	1475		S–C–H bend	1178	1135
B_2	C–H stretch	3025	3028	3217	3023	3212	3061		S–H stretch	2376	2261
	S–C–H bend	(1438)	991	1051	968	1040	976		C–H stretch	2813	2816
B_1	out-of-plane	(1110)	990	1014	1029	1120	1036	A″	out-of-plane	812	779

[a] Calculated HF/3-21G frequencies scaled by 0.9. [b] Reference 29. [c] See ref 30. [d] Reference 49, at CEPA geometry. [e] Scaled DZ+d harmonic frequencies, ref 53.

The trans conformer of HCSH lies slightly lower in energy than the cis form at all levels of treatment, the energy differences ranging from 3.4 kcal/mol (HF/3-21G//3-21G) to 2.1 kcal/mol (MRDCI/TZ+2d1p//TZ+d). The addition of polarization functions and incorporation of electron correlation both slightly favor the cis form, hence reducing the energy separation from the HF/3-21G//3-21G value.

The SH and CH bond distances in the isomeric thiohydroxycarbenes are similar, with values comparable to those calculated for H_2S and CH_2.[88] The calculated CS bond length of 1.67 Å is considerably shorter than a single CS bond distance, such as the value of 1.81 Å (experimental) in thiomethanol, suggesting the CS bond in thiohydroxycarbene has some double-bond character.

For the cis form the SCH and CSH angles open up by 6.2 and 6.6°, respectively, with the SH bond lengthening slightly to relieve steric hindrance between the hydrogens.

The multiple bond character of the CS bond in HCSH is further suggested by the geometry of the rotational transition state and the height of the barrier to rotation. The relaxed rotation involves

a transition state with a CS bond length of 1.837 Å at a conformation in which the CH and SH bonds are nearly orthogonal, with a dihedral angle of 89.5° in a system where by convention the cis species is defined to have a dihedral angle of zero. The observed lengthening of the CS bond by some 0.16 Å relative to thiohydroxycarbene may be related to the destruction of π-bonding between carbon and sulfur upon distortion of the system from planarity. At the HF/3-21G//3-21G level the calculated barrier to rotation is 24.6 kcal/mol. Incorporation of polarization functions and electron correlation raises this barrier by 8.9 and 7.0 kcal/mol, respectively, resulting in a final MRDCI/TZ+2d1p//TZ+d value of 41.1 kcal/mol.

Calculations at the HF/3-21G//3-21G level on a structure with the CSH group linear indicated that the energy required for inversion at the carbene center is significantly greater than that for rotation.

The transition state (**5**) for the 1,2-hydrogen shift rearrangement of thioformaldehyde to *trans*-thiohydroxycarbene is predicted to be planar and is seen to more closely resemble *trans*-HCSH than H_2CS, particularly in the CS bond length. This is in line with Hammond's postulate[89] for a reaction which is strongly endothermic in the direction $H_2CS \rightarrow$ *trans*-HCSH. The predicted barrier height as a function of treatment displays the usual phenomena in that successively smaller barriers result from increasing theoretical sophistication. The barrier for the rearrangement of thioformaldehyde is 109.6 kcal/mol at the HF/3-21G//3-21G level. Extending the s,p basis reduces the barrier to 104.3 kcal/mol (HF/TZ), while the addition of polarization functions reduces it still further to 92.9 kcal/mol. A further decrease of 4.4 kcal/mol is found at the MRDCI/TZ+2d1p//TZ+d level, leading to an estimate of 88.5 kcal/mol. This is equivalent to a barrier of 39.8 kcal/mol for the reverse process, *trans*-HCSH $\rightarrow$ H_2CS. Corresponding values of 88.0 and 40.8 kcal/mol are obtained at the SDCI level. The generalized unlinked cluster correction yields values of 84.5 and 37.4 kcal/mol, respectively.

Scaled vibrational frequencies for *cis*- and *trans*-HCSH, determined at the HF/3-21G//3-21G level, are given in Table VI. Although the highest frequency mode, corresponding to C–H stretch, is the same in both isomers, values of the S–H stretch are reasonably well separated (2376 cm^{-1}, trans; 2261 cm^{-1}, cis), suggesting that it may be possible to identify both isomers experimentally by their infrared spectra, assuming they can be isolated. Note also that the C–H stretch is quite different from those of thioformaldehyde, the most likely precursor in thiohydroxycarbene synthesis. The significantly longer S–H bond in the cis isomer (+0.013 Å) is reflected by the smaller S–H frequency relative to the trans form, while the decrease in the C–S stretch relative to H_2CS is associated with the significantly longer C–S bond in both isomers (cis, 1.666 Å; trans, 1.675 Å) compared to that in thioformaldehyde (1.600 Å). Vibrational frequencies determined for the rearrangement transition state (**5**) reveal a scaled imaginary frequency of 2343*i* cm^{-1} associated with the reaction coordinate indicating, just as in the formaldehyde rearrangement,[20] a fairly thin barrier through which tunnelling may be important. The frequency associated with the reaction coordinate in the rotation transition state (**4**) is, as expected, significantly smaller, with a HF/3-21G//3-21G value of 840*i* cm^{-1}.

The zero-point energy difference (see Table IV) causes the calculated H_2CS to *trans*-HCSH rearrangement barrier to decrease by 5.3 kcal/mol, in line with the decrease of 4.2 kcal/mol found in the corresponding formaldehyde rearrangement. Zero-point differences lead to a decrease of 2.7 kcal/mol in the computed barrier for the reverse reaction, *trans*-HCSH $\rightarrow$ H_2CS. The calculated trans–cis rotational barrier is reduced by 1.9 kcal/mol on allowing for zero-point effects.

C. Molecular Dissociation of Thioformaldehyde. Total energies and geometrical parameters of the dissociation products H_2 and CS, and of the transition state (**6**) for molecular dissociation at various levels of theoretical treatment, are given in Tables IV and III, respectively. In contrast to the effectively thermoneutral molecular dissociation of formaldehyde,[20] the dissociation of thioformaldehyde ($^1A_1$, S_0) to ground-state molecular products, H_2 ($^1\Sigma_g^+$) and CS ($^1\Sigma^+$), is predicted to be endothermic at all levels of treatment. The predicted dissociation energy is seen to decrease steadily with successive improvements in the theoretical method employed, with the HF/3-21G//3-21G value of 56.7 kcal/mol decreasing to 30.6 kcal/mol when applying the PSK and ZPVE corrections to the MRDCI/TZ+2d1p//TZ+d estimate.

The 3-21G energy barrier for the dissociation of thioformaldehyde to the molecular products via the planar transition state was calculated to be 119.7 kcal/mol. Increasing the flexibility of the basis set, with extension of the s,p space and introduction of polarization functions leads to a decrease in the barrier, arising from a better description of the highly distorted molecular transition state. Thus the HF/TZ+2d1p//TZ+d barrier is reduced to 104.1 kcal/mol. A further decrease is found upon incorporation of electron correlation, with the SDCI and MRDCI calculations lowering the energy barrier by 6.3 and 6.2 kcal/mol, respectively. Our best estimate of the barrier determined as the difference between two variationally calculated energies is 97.9 kcal/mol. Using the PSK correction to estimate the contribution from unlinked clusters leads to a further reduction in the barrier height of 2.4 kcal/mol at the SDCI level and 2.7 kcal/mol at the MRDCI level of treatment. A barrier of 61.3 kcal/mol for the reverse process, the molecular reaction of H_2 and CS to form thioformaldehyde, is given at the MRDCI level, a value which decreases to 57.0 kcal/mol upon inclusion of the quadruples correction.

Both the HF and CI energies from our most extensive calculations on the $X^1\Sigma^+$ state of CS are lower than those previously reported.[90-94] A significant decrease in C–S bond length is found with basis set extension, the HF/3-21G value of 1.564 Å decreasing to 1.518 Å at the HF/TZ+d level, a value slightly smaller than experiment (1.534 Å).[95]

The geometry of the molecular transition state is similar to that determined in the molecular dissociation of formaldehyde.[20] Thus both hydrogens lie on the same side of the C–S axis in a planar structure, with one C–H bond significantly elongated and the other slightly stretched relative to their values in the ground-state molecule. This unequal stretching of the bonds allows the system to avoid what is an orbitally forbidden process in C_{2v} symmetry,[96] although the substantial distortion energy required to attain the lower C_s symmetry leads to a high barrier. The H–H distance of 0.929 Å derived from the TZ+d calculations is large compared to the equilibrium bond length of the product H_2 (0.742 Å[97]), while the C–S distance of 1.594 Å is, in apparent violation of Hammond's postulate, much closer to that in thioformaldehyde than in the product CS molecule.

The scaled vibrational frequency associated with the reaction coordinate in the transition state is 2030*i* cm^{-1}, suggesting the barrier is fairly thin and sharp, as well as being quite high. A final value of 89.0 kcal/mol is given for the PSK corrected MRDCI/TZ+2d1p//TZ+d barrier on allowing for zero-point vibrational energies of 9.8 and 16.7 kcal/mol for the molecular transition state and parent molecule, respectively. A calculated ZPVE of 8.3 kcal/mol for the molecular dissociation products causes a slight increase in the potential barrier to molecular formation, with a final MRDCI+QC+ZPVE estimate to 58.4 kcal/mol.

D. Radical Dissociation of Thioformaldehyde. Calculations on the dissociation of H_2CS (S_0) to atomic hydrogen plus the

(89) Hammond, G. S. *J. Am. Chem. Soc.* **1955**, *77*, 334.
(90) Bruna, P. J.; Kammer, W. E.; Vasudevan, K. *Chem. Phys.* **1975**, *9*, 91.
(91) Richards, W. G. *Trans. Faraday Soc.* **1967**, *63*, 257.
(92) Green, S. *J. Chem. Phys.* **1971**, *54*, 827.
(93) Raine, G. P.; Schaefer, H. F.; Haddon, R. D. *J. Am. Chem. Soc.* **1983**, *105*, 194.
(94) Goddard, J. D. *Chem. Phys. Lett.* **1983**, *102*, 224.
(95) Mockler, R. C.; Bird, G. R. *Phys. Rev.* **1955**, *98*, 1837.
(96) Pearson, R. G. "Symmetry Rules for Chemical Reactions"; Wiley-Interscience: New York, 1976; p 508.
(97) Herzberg, G. "Spectra of Diatomic Molecules"; Van Nostrand: Princeton, 1950.

Table VII. GVB-1/PP/TZ+d Calculations on the Radical Dissociation of Thioformaldehyde (X^1A_1)[a]

$r(C-H_1)$	total energy	$r(C-S)$	$r(C-H_2)$	$\angle H_1CS$	$\angle H_2CS$
5.00	−436.408 15	1.556	1.077	126.4	134.8
3.00	−436.411 15	1.556	1.076	126.4	135.1
2.50	−436.420 15	1.557	1.074	124.9	134.9
2.00	−436.448 45	1.565	1.073	123.3	132.4
1.75	−436.475 17	1.573	1.073	122.9	129.8
1.50	−436.510 63	1.585	1.073	122.9	126.6
1.30	−436.540 31	1.593	1.076	122.4	124.3
1.10	−436.556 70	1.600	1.078	122.0	122.6
1.075	−436.556 36	1.600	1.078	122.1	122.4

[a] Energies in hartrees; all distances in Å; angles in deg.

thioformyl radical (HCS, $^2A'$) were conducted using a two-configuration SCF wave function (GVB-1/PP[98]), the minimum level at which a qualitative description of the radical dissociation pathway might be realized.[15] This pathway was mapped out by fixing the distance of the dissociating hydrogen (H_1) from the carbon of H_2CS, and optimizing the remaining geometrical parameters assuming the hydrogen atom departs in the HCS plane.[15] The total energies for points along this pathway determined at the GVB-1/PP/TZ+d//GVB-1/PP/TZ+d level are given in Table VII. At the thioformaldehyde equilibrium geometry, the GVB-1 result is 0.0163 hartree below the HF/TZ+d result. With the departing hydrogen 5.0 Å away from the carbon, the GVB-1 curve becomes flat at an energy corresponding to that of H and HCS ($^2A'$) (see section 5.4).

Total energies derived from SCF and CI calculations on the separated radicals are given in Table IV. The dissociation energy is seen to decrease somewhat at the SCF level upon improving the basis set, with a HF/TZ+2d1p//TZ+d estimate of 83.7 kcal/mol. In contrast to the molecular dissociation of H_2CS, and the radical dissociation of H_2CO,[15] the incorporation of electron correlation is seen to increase the dissociation energy (93.2 kcal/mol from the MRDCI + QC treatment), although this increase is largely offset by ZPVE corrections. Thus at the MRDCI+QC+ZPVE level the energy requirement of 85.2 kcal/mol for radical dissociation on the S_0 surface is predicted to be slightly smaller than the value of 89.0 kcal/mol determined for the molecular dissociation process.

5.2 Dissociation and Rearrangements on the T_1 Potential Energy Surface of H_2CS. Total energies as a function of treatment for the $^3A''$ state of H_2CS (T_1, **7**), the lowest triplet state of thiohydroxycarbene (^3A, **8**) and the transition state (**9**) for the 1,2 hydrogen shift H_2CS (T_1) → HCSH (T_1) are given in Table IV. For convenience calculations on the $^1A''$ state are also considered at this point. Geometries for the various species obtained at the 3-21G, TZ, and TZ+d HF levels are given in Table III.

The calculated transition energies reveal the usual behavior at the Hartree–Fock level,[88] with the X^1A_1–a^3A'' and X^1A_1–A^1A'' splittings significantly underestimated. Thus the HF/TZ+2d1p//TZ+d values of 25.7 and 29.9 kcal/mol for the triplet and singlet splittings, respectively, are some 16 kcal/mol smaller than experiment.[35,36] Incorporation of electron correlation largely remedies this situation, with the MRDCI/TZ+2d1p//TZ+d values of 41.8 and 47.2 kcal/mol, respectively, within 0.5 kcal/mol of the splittings obtained by Judge and King.[35] Zero-point and unlinked cluster corrections cancel between the ground and excited states, with the ZPVE correction decreasing and the quadruples correction increasing the splitting for the $^3A''$ state, by 1.5 and 1.8 kcal/mol, respectively. The discrepancy of 4 kcal/mol between the SDCI+QC+ZPVE transition energies and experiment is consistent with the significant increase in ΔE predicted in the MRDCI as compared to the SDCI treatment.

The elongation of the C–S bond expected to accompany an n → π^* electron promotion is seen to decrease slightly with basis set improvement, with the HF/3-21G lengthening of 0.17 Å in the $^3A''$ state decreasing to 0.14 Å at the TZ+d level. The TZ+d geometry of the a^3A'' state is almost identical with the DZ** optimized geometry of ref 53; slightly poorer agreement with the experimental r_0 structure[40] is found compared to the ground-state calculations, with the C–S bond length overestimated in the triplet state by 0.050 Å (experimental $r(C-S) = 1.683 \pm 0.005$ Å). The computed out-of-plane angle of 21.0° (TZ+d) is in agreement with a previous estimate of 20.7°.[53] The smaller value of 15.9° from ref 47 is not surprising in view of the very low inversion barrier, for thioformaldehyde would appear to be "floppy planar" in both the $^3A_2$ and $^1A_2$ states. An estimate of the barrier to planarity of 7 cm^{-1} has been given for the triplet state,[39] while use of the semirigid invertor Hamiltonian suggests a planar structure for the singlet state. The situation is certainly very different from the corresponding electronic states in formaldehyde, where barriers to planarity are 316 and 762 cm^{-1}, respectively, for the excited triplet and singlet states.[39]

The equilibrium geometry of the lowest triplet state of HCSH is found to be a gauche nonplanar structure (**8**), in line with the qualitative structure found for the lowest triplet state of hydroxycarbene.[12] The calculated CS bond length, 1.737 Å at the TZ+d level, is found to be identical with that in H_2CS (T_1). Calculations at the SDCI/TZ+2d1p//TZ+d level produced energies of −436.78306 and −436.74524 hartrees for H_2CS (T_1) and HCSH (T_1), respectively, giving an energy difference of 23.8 kcal/mol; unlinked cluster and zero-point vibrational corrections reduce the separation somewhat to 22.5 kcal/mol. At this level of theory the ^3A state is predicted to lie 15.4 kcal/mol above the $^1A'$ state of the trans configuration, a significant increase in the separation of only 1.7 kcal/mol predicted at the HF/TZ+2d1p//TZ+d level.

The barrier height for the H_2CS (T_1) → HCSH (T_1) rearrangement follows the general pattern, as a function of level of theory, found in the corresponding rearrangement on the S_0 surface (section 5.1B) and in previous calculations of 1,2 hydrogen shifts.[22,99-102] Both the addition of polarization functions and the inclusion of correlation effects act to lower the predicted barrier height, yielding a final corrected (SDCI+QC+ZPVE) estimate of 45.7 kcal/mol. Of some note is the large difference (0.106 Å) between the 3-21G and TZ+d predictions of the CS distance in the transition structure.

Minimal basis set calculations on the radical dissociation of formaldehyde on the T_1 surface suggest, in contrast to the S_0 surface, the presence of a barrier 9.2 kcal/mol[69] above H and HCO in their ground states. The presence of such a barrier was important in determining that H_2CO dissociates to radical products on the S_0, rather than the T_1 surface. Corresponding calculations on the T_1 surface of thioformaldehyde yield a transition structure (**10**), with an anticipated long CH bond (1.732 Å). This structure lies 10.6 kcal/mol above the dissociation products at the HF/TZ+2d1p//TZ+d level, zero-point corrections increasing this estimate to 12.3 kcal/mol. The barrier is significantly reduced, however, when electron correlation is taken into account, with our best estimates being 2.2 kcal/mol at the SDCI/TZ+2d1p//TZ+d level, and only 0.6 kcal/mol when allowing for both zero-point vibration and unlinked cluster corrections.

5.3 Features of the Potential Energy Surface of H_2CS^+, the Thioformaldehyde Cation. The total and relative energies of the $^2B_2$ (**11**) and $^2B_1$ states of H_2CS^+, the trans (**12**) and cis (**13**) isomers of the thiohydroxycarbene cation ($HCSH^+$), and the 1,2-hydrogen shift $H_2CS^+(^2B_2)$ → *trans*-$HCSH^+$ ($^2A'$) rearrangement transition state (**14**) are given in Tables IV and VIII, respectively. Optimized geometries for each species are listed in Table III. The calculated adiabatic IPs reveal the expected behavior at the SCF level, with the HF/TZ+2d1p//TZ+d values

(98) Bobrowicz, F. W.; Goddard, W. A., III, In "Modern Theoretical Chemistry"; Schaefer, H. F., III, Ed.; Plenum Press: New York, 1977; Vol. 3, p 79.

(99) Demuynck, J.; Cox, D. J.; Yamaguchi, Y.; Schaefer, H. F. *J. Am. Chem. Soc.* **1980**, *102*, 6204.

(100) Schaefer, H. F. *Acc. Chem. Res.* **1979**, *12*, 288.

(101) Nobes, R. H.; Radom, L.; Rodwell, W. R. *Chem. Phys. Lett.* **1980**, *74*, 269.

(102) Krishnan, R.; Frisch, M. J.; Pople, J. A.; Schleyer. P. v. R. *Chem. Phys. Lett.* **1981**, *79*, 408.

Table VIII. Calculated Relative Energies (kcal/mol) for H_2CS^+ and Component Systems

species	sym-metry	electronic state	HF/TZ //TZ	HF/TZ+2d1p //TZ+d	SDCI/TZ+2d1p //TZ+d	MRDCI/TZ+2d1p //TZ+d	SDCI + ZPVE + QC	MRDCI + ZPVE
H_2CS^+ (**11**)	C_{2v}	$^2B_2$	0.0	0.0	0.0	0.0	0.0	0.0
H_2CS^+	C_{2v}	$^2B_1$	36.9	42.7	51.1			
trans-$HCSH^+$ (**12**)	C_s	$^2A'$	43.9	29.7	32.3	32.5	30.2	30.5
cis-$HCSH^+$ (**13**)	C_s	$^2A'$	46.2	31.2	34.5	34.7	32.3	32.3
TS (**11** → **12**) (**14**)	C_s	$^2A'$	89.0	71.1	61.9	61.6	55.4	56.7

Table IX. Calculated Relative Energies (kcal/mol) for HCS, HCS^+, and Component Systems[a]

species	sym-metry	electronic state	HF/TZ //TZ	HF/TZ+2d1p //TZ+d	SDCI/TZ+2d1p //TZ+d	MRDCI/TZ+2d1p //TZ+d	SDCI + ZPVE + QC	MRDCI + ZPVE
HCS (**15**)	C_s	$^2A'$	0.0	0.0	0.0	0.0	0.0	0.0
TS (**15** → H + CS) (**16**)	C_s	$^2A'$	59.2	53.3	51.5	51.3	43.9	46.5
CSH (**17**)	C_s	$^2A'$	36.5	30.9	39.0	42.1	38.1	40.4
TS (**15** → **17**) (**18**)	C_s	$^2A'$	77.5	66.7	63.2	64.7	58.3	61.0
H + CS			50.9	43.9	51.0	49.1	46.5	43.7 (44.9)
HCS^+ (**19**)	$C_{\infty v}$	$^1\Sigma^+$	0.0	0.0	0.0	0.0	0.0	0.0
CSH^+ (**20**)	C_s	$^1A'$	76.1	68.6	75.1	77.8	71.1	74.2
TS (**19** → **20**) (**21**)	C_s	$^1A'$	94.0	78.3	77.7	79.0	71.0	73.7
H + CS^+			125.7	123.9	137.5	136.6	131.0	129.8 (129.2)
H^+ + CS			187.0	193.4	196.6	198.4	189.2	191.4 (189.6)

[a] Values in parentheses include generalized QC contribution (MRDCI+QC+ZPVE).

of 8.28 and 10.13 eV for the $3b_2$ and $2b_1$ IPs underestimating experiment by 1.06 and 1.76 eV, respectively. These discrepancies are reduced to 0.33 and 0.58 eV when electron correlation is included at the SDCI + QC level, yielding calculated IPs of 9.01 (b_2) and 11.31 eV (b_1). Our best values are consistent with previous calculations of the vertical IPs, notably CI estimates of 9.08 and 11.49 eV,[33] and the values of 9.12 and 11.63 eV obtained using a many-body Greens function method.[51] Indeed the calculations of von Niessen et al.[51] suggest that extensions to the basis set, with the addition of f functions, and a more diffuse d orbital would be required for better agreement with experiment.

The geometry changes accompanying ionization of H_2CS are consistent with the ideas of qualitative molecular orbital theory. Thus ionization from the sulfur lone-pair orbital, the $3b_2$ (n) MO, results in effectively no distortion of the CS bond. In contrast, ionization from the CS π-bonding orbital, the $2b_1$ MO, leads to a significant lengthening of the C–S distance, with the HF/TZ+d estimate of 1.600 Å for the neutral molecule increasing to 1.732 Å in the $^2B_1$ ion.

Significant changes in the CS bond length of thiohydroxycarbene are also predicted upon ionization, with the HF/TZ+d bond length of 1.675 Å in the $^1A'$ neutral trans isomer reduced by 0.08 Å in trans $HCSH^+$. The present calculations predict a first IP of 7.72 eV for the trans isomer at the HF level, which increases to 8.39 eV when electron correlation is included. Previous calculations on the formaldehyde and hydroxycarbene radical cations[104-106] suggest that H_2CO^+ ($^2B_2$) is more stable than the low-energy trans configuration of $HCOH^+$. Estimates of 5.5 and 3.6 kcal/mol have been reported for this separation by Osamura et al.[103] and Frisch et al.,[104] both studies including electron correlation. A somewhat larger value of 9.7 kcal/mol is obtained at the HF level.[105] These values are significantly smaller than the corresponding energy separation of the neutral species (55.7 kcal/mol[104]). As might be expected, the present results show a similar, but somewhat less pronounced trend. H_2CS^+ is predicted to be more stable than $HCSH^+$ by 30.2 kcal/mol at the SDCI+QC+ZPVE level (Table VIII), as compared with the neutral molecule separation of 44.8 kcal/mol at the same level of theory (Table V). An estimate of "about 1 eV" for the $H_2CS^+/HCSH^+$ separation has been deduced from photoionization mass spectrometric measurements.[60]

The cis form of the thiohydroxycarbene radical cation (**13**) is found to be 2.0 kcal/mol higher in energy than the trans form (**12**), an energy difference similar to that found for the neutral species (1.7 kcal/mol, Table V). Somewhat larger separations have been found for hydroxycarbene, with values of 4.8 and 4.1 kcal/mol reported for the neutral and ionic systems, respectively. The barrier of 25.2 kcal/mol for the rearrangement of *trans*-$HCSH^+ \rightarrow H_2CS^+$ is sufficient to suggest that $HCSH^+$ would have a finite lifetime. A significantly higher barrier of 59 kcal/mol has been calculated[105] for the oxygen analogue process *trans*-$HCOH^+ \rightarrow H_2CO^+$. As in the neutral molecule rearrangements on the S_0 and T_1 surfaces, we find a steady decrease in the barrier height for the 1,2 hydrogen shift as the level of treatment is improved.

5.4 Thioformyl Radical. Total and relative energies for the stationary points on the potential energy surface of the thioformyl radical, HCS, are given in Tables IV and IX, respectively. Equilibrium structures of the HCS (**15**) and CSH (**17**) isomers, of the transition state for their interconversion (**18**), and for the process HCS → H+CS (**16**) are given in Table III.[106]

The ground-state electronic configuration of the thioformyl radical is X^2A' (. . .$6a'^2 7a'^2 8a'^2 9a'^2 2a''^2 10a'$), with the 10a' orbital of largely carbon lone-pair character at the equilibrium geometry. As the CH bond length increases, this orbital localizes on the hydrogen atom, becoming a 1s H orbital upon dissociation, while the remaining orbitals asymptotically approach the HF orbitals of CS. Thus the HF wave function of HCS dissociates correctly. Since this configuration is also the ground state for the CSH isomer, the HF method can be expected to provide a reasonable zeroth-order description of the equilibrium structures of HCS and HSC, the dissociation of these species to H and CS, and the isomerization of HSC to HCS.

In line with previous studies of mixed first- and second-row HAB molecules,[107,108] we find the more stable isomer to be that with the terminal position occupied by the heavier atom. The calculated TZ+d equilibrium angle of 134.6° in the thioformyl radical is consistent with the value of 127.4° in the formyl radical,[109] while the C–S bond length of 1.557 Å is intermediate in

(103) Osamura, Y.; Goddard, J. D.; Schaefer, H. F.; Kim, K. S. *J. Chem. Phys.* **1981**, *74*, 617.
(104) Frisch, M. J.; Raghavachari, K.; Pople, J. A.; Bouma, W. J.; Radom, L. *Chem. Phys.* **1983**, *75*, 323.
(105) Bouma, W. J.; MacLeod, J. K.; Radom, L. *Int. J. Mass Spectrom. Ion Phys.* **1980**, *33*, 87.
(106) In spite of repeated attempts, we were unable to locate a transition state for the process CSH → CS + H, suggesting, in contrast to the formyl radical, the absence of a barrier for this process at the HF level.
(107) Bruna, P. J.; Hirsch, G.; Buenker, R. J.; Peyerimhoff, S. D. In "Molecular Ions: Geometric and Electronic Structures"; NATO ASI Series; Plenum Press: New York, 1982.
(108) Buenker, R. J.; Bruna, P. J.; Peyerimhoff, S. D. *Isr. J. Chem.* **1980**, *19*, 309.

value between that in CS (1.518 Å) and thioformaldehyde (1.600 Å). The H–CS bond energy of 43.9 kcal/mol determined at the HF/TZ+2d1p//TZ+d level increases upon incorporation of electron correlation, with estimates of 51.0 and 49.1 at the SDCI and MRDCI levels, respectively. These values, modified by both quadruples and ZPVE corrections, suggest a significantly stronger H–C bond than in the formyl radical (18.7 ± 1.5 kcal/mol[110]), a conclusion which is in accord with the calculated C–H bond lengths of 1.077 (HF/TZ+d) and 1.120 Å[111] in HCS and HCO, respectively. The HF/TZ+d geometry is in excellent agreement with that derived at the HF/DZ+P level.[94] Geometry optimization at the SDCI level is found to predict a decrease of 2° in the HCS angle, with the C–S and C–H distances increasing by 0.011 and 0.006 Å, respectively, with respect to the SCF values.[94] Total SCF and MRDCI values from the present study are 3.9×10^{-2} and 7.7×10^{-2} hartree below the corresponding values of ref 94.

Calculations on the dissociation transition state (**16**) show that the CH bond has stretched by 0.66 Å, while both the C–S bond length and the HCS bond angle have decreased, with the bond just 0.009 Å longer than that of the diatomic molecule. The calculated barrier at the HF/TZ+2d1p//TZ+d level for this process is 53.3 kcal/mol, with the transition state 9.4 kcal/mol above the dissociation products. These values may be compared with the values of 22.7 and 5.7 kcal/mol for the formyl radical.[111] Upon incorporation of electron correlation, however, the barrier to molecular formation is reduced to just 2.2 kcal/mol at the MRDCI level, zero-point corrections increasing this value somewhat to 2.8 kcal/mol. These values suggest that the reaction between H and CS would occur spontaneously.

The calculated vibrational frequencies at the transition state are 1261, 441, and 1413*i* cm^{-1}, the real frequencies corresponding to CS stretch and HCS bend, the imaginary frequency to transmission over the barrier.

Turning to the CSH species, we obtain a HF isomerization energy of 30.9 kcal/mol, correlation effects increasing this value to 42.1 kcal/mol at the MRDCI level. The less stable isomer is found to exhibit a significantly longer CS bond (1.679 Å compared with 1.557 Å) and a somewhat more acute bond angle (100.9°) than in the parent species. The calculated CS–H bond energy of 4.5 kcal/mol at the MRDCI+QC+ZPVE level suggests that HSC is bound with respect to loss of atomic hydrogen, in contrast to the less stable isomer of the formyl radical.[111] At the saddle point (**18**) for isomerization the HCS angle is 54.2°, while the SH and CS bond lengths of 1.439 and 1.678 Å, respectively, are similar to those found in the less stable isomer. The relative energies of Table IX reveal that the barrier to isomerization (20.2 kcal/mol at the SDCI+QC+ZPVE level) exceeds the dissociation estimate by some 10.8 kcal/mol. The absence of a barrier for the process CSH → CS + H[106] would suggest that isomerization occurs via a two-step mechanism, involving dissociation of HSC and recombination to form HCS.

5.5 Thioformyl Cation, HCS^+. Total and relative energies for stationary points on the potential energy surface of the thioformyl cation, HCS^+, are given in Tables IV and IX, respectively. Equilibrium structures of the HCS^+ (**19**) and CSH^+ (**20**) isomers, and of the transition state (**21**) for their interconversion are given in Table III.

The ground-state electronic configuration of the HCS^+ isomer is $^1\Sigma^+(\ldots 6\sigma^2 7\sigma^2 1\pi^4)$. In agreement with a previous MRDCI study[112] of the HCS^+–HSC^+ system, we find the C–S bond to be shorter in HCS^+ than in CS itself, but to be increased by some 0.09 Å relative to the diatomic species in the CSH^+ isomer.

Values of 123.9 and 136.6 kcal/mol for the dissociation energy of HCS^+ relative to a hydrogen atom and the CS^+ ion at the HF/TZ+2d1p//TZ+d and MRDCI+QC levels are significantly smaller than previous estimates of 154.8 and 163.8 kcal/mol.[112] This discrepancy of some 30 kcal/mol would largely account for the differing estimates of $\Delta H_{f,0}(HCS^+)$ deduced from experiment (259.2 ± 0.1[60] and 256 ± 4.5 kcal/mol[113]) and previous calculations (220 ± 5 kcal/mol at the CI level[112]), although a recent photoionization study has suggested a somewhat lower value of 233 kcal/mol.[114] The MRDCI+QC+ZPVE estimate of 189.6 kcal/mol for the proton affinity of CS is in reasonable agreement with the experimental value of 174.5 ± 4.5 kcal/mol,[113] while the MRDCI+QC value of 10.97 eV for the ionization potential of the CS molecule compares favorably with the experimental estimate of 11.33 eV,[115] with ionization leading to a decrease of 0.059 Å in the C–S distance.

The previous MRDCI study suggested that the CSH^+ isomer is unstable, there being no barrier to rotation of the H atom from the sulfur to the carbon side of the C–S bond. Calculations on the respective linear conformations predicted CSH^+ to be some 110 kcal/mol less stable than HCS^+, suggesting, in fact, that the less stable isomer corresponded to a saddle point on the potential energy surface.[112] The present calculations at the HF level predict that CSH^+ does, in fact, correspond to a minimum, with a strongly bent structure lying some 68.6 kcal/mol above the more stable isomer at the HF/TZ+2d1p//TZ+d level. These findings are in agreement with the calculations of Berthier et al.,[116] who predicted an energy separation of 72 kcal/mol with a strongly bent HSC^+ structure. A significant barrier to isomerization is found at the lower levels of treatment (see Table IX), with the TZ+d saddle point (**21**) characterized by an HCS angle of 71.1° and C–H and C–S distances of 1.281 and 1.534 Å, respectively. The incorporation of polarization functions is seen to lower the barrier from 17.9 kcal/mol (HF/TZ//TZ) to 9.7 kcal/mol (HF/TZ+2d1p//TZ+d). Electron correlation acts to reduce the barrier still further, with SDCI and MRDCI estimates of 2.6 and 1.2 kcal/mol, respectively. The inclusion of both unlinked cluster and zero-point corrections results in the transition structure lying 0.5 kcal/mol *below* the HSC^+ cation. While casting some doubt on the HF predictions for the HSC^+ minimum, the present results are in broad agreement with those of ref 112 in suggesting that the 1,2 hydrogen shift occurs without activation energy.

6. Conclusions

The present work provides the first consistent and detailed study of the transition-state geometries and barrier heights of thioformaldehyde on both its S_0 and T_1 surfaces, with calculations on the dissociation to both molecular and radical products, and on the intramolecular rearrangement to thiohydroxycarbene. The computed values for the S_0–S_1 and S_0–T_1 adiabatic excitation energies are found to be in good agreement with experiment: the MRDCI estimates of 41.8 and 47.2 kcal/mol compare favorably with the experimental values of 41.5 and 46.8 kcal/mol, respectively. Our best computed estimates (MRDCI+QC+ZPVE) for the molecular and radical dissociation energies on the S_0 surface of 30.6 and 85.2 kcal/mol, respectively, compare less satisfactorily with the corresponding experimental data of 40.0 and 91.4 kcal/mol.[24] However, these latter values are based on limited thermochemical data and are considered as only approximate.[56] Although molecular dissociation of H_2CS appears to be thermodynamically feasible upon excitation to the S_1 state, the failure to observe photodissociation is readily explained by the presence of a high activation barrier, 89.0 kcal/mol, at the MRDCI+QC+ZPVE level, as compared with the $S_0 \rightarrow S_1$ excitation energy of just 45.7 kcal/mol.

As in formaldehyde the energy requirements for radical and molecular dissociation are very similar, our best values being 85.2 and 89.0 kcal/mol, respectively. Furthermore, the energy required for molecular rearrangement to thiohydroxycarbene (79.2 kcal/mol) is evidently of the same order of magnitude as that required for dissociation. The present calculations provide a firm

(109) Austin, J. A.; Levy, D. H.; Gottlieb, C. A.; Redford, H. E. *J. Chem. Phys.* **1974**, *60*, 207.
(110) Warneck, P. *Z. Naturforsch. A* **1974**, *29*, 350.
(111) Dunning, T. H., Jr. *J. Chem. Phys.* **1980**, *73*, 2304.
(112) Bruna, P. J.; Peyerimhoff, S. D.; Buenker, R. J. *Chem. Phys.* **1978**, *27*, 33.
(113) McAllister, T. *Astrophys. J.* **1978**, *225*, 857.
(114) Butler, J. T.; Baer, T. *J. Am. Chem. Soc.* **1982**, *104*, 5016.
(115) Jonathan, N.; Morris, A.; Okuda, M.; Ross, K. J.; Smith, D. J. *Discuss. Faraday Soc.* **1972**, *54*, 48.
(116) Berthier, G.; Pauzat, F.; Yuangi, T. *J. Mol. Struct.* **1984**, *107*, 39.

prediction of the viability of thiohydroxycarbene. It is clear that the energetic dispositions of the stationary points on the S_0 potential energy surface of thioformaldehyde are in many instances similar to those on the ground-state surface of formaldehyde. Theory suggests[22] that the activation energy for $H_2CO \rightarrow H_2 + CO$ is about 80 kcal/mol, while that for isomerization to hydroxycarbene is about 81 kcal/mol. Clearly the much lower excitation energy for the $^1A_2(S_1)$ state of H_2CS compared to that of H_2CO (80.6 kcal/mol) accounts for the failure to observe photodissociation as an important decay process for H_2CS in its first excited singlet state. As noted previously, this is consistent with LPE[42] and LOAD[36] spectra, where strong emission from highly excited vibrational levels of the A^1A_2 state is observed, in marked contrast to formaldehyde, where dissociation processes become increasingly dominant with increasing energy, resulting in a breakoff in the fluorescence excitation spectrum.

Our best computed estimates of the barrier for dissociation of H_2CS ($^3A''$) to H + HCS ($^2A'$) and for isomerization to HCSH (^3A) on the T_1 surface are 50.4 and 45.7 kcal/mol, respectively, with the ^3A HCSH excited state lying 15.4 kcal/mol above the $^1A'$ state of *trans*-HCSH.

Calculations on the potential energy surface of the thioformaldehyde cation predict H_2CS^+ ($^2B_2$) to be 30.2 kcal/mol more stable than *trans*-$HCSH^+$ ($^2A'$), in good agreement with the separation deduced from photoionization mass spectrometric measurements.[60] A barrier of 55.4 kcal/mol is computed for the rearrangement of H_2CS^+ to the less stable isomer.

The study of the potential energy surface of the thioformyl radical suggests that the HSC → HCS ($^2A'$) isomerization occurs via a two-step mechanism, involving dissociation of HSC and recombination to form the more stable isomer. The corresponding 1,2 hydrogen shift in the thioformyl cation is predicted to occur without activation energy.

Registry No. H_2CS, 865-36-1; $H_2DS^{+\cdot}$, 61356-81-8; $HCS^{\cdot}$, 36058-28-3; HCS^+, 59348-25-3.

Theoretical Determination of Molecular Structure and Conformation. 15. Three-Membered Rings: Bent Bonds, Ring Strain, and Surface Delocalization

Dieter Cremer* and Elfi Kraka

Contribution from the Lehrstuhl für Theoretische Chemie, Universität Köln, D-5000 Köln 41, West Germany. *Received October 10, 1984*

Abstract: Energy, geometry, one-electron density distribution, and Laplace concentrations of cyclopropane (**1**), aziridine (**2**), oxirane (**3**), cyclopropyl anion (**4**), protonated aziridine (**5**), protonated oxirane (**6**), halogen-bridged fluoroethyl cation (**7**), and hydrogen-bridged ethyl cation (**8**) are investigated and compared with their corresponding alicyclic counterparts. The relationship between three-membered rings (3MR) and π-complexes is demonstrated by analyzing their electron density pattern with the aid of catastrophe theory. A continuous change from 3MRs to π-complexes can be observed if the acceptor (donor) ability of a group X interacting with an ethylene unit is increased (decreased). The bend of the 3MR bonds is described by the curvature of the paths of maximum electron density linking the ring atoms. Interpath angles are used to evaluate the strain energy of a 3MR. A value of 75 kcal/mol is found for **1**. Strain is partially compensated by stabilizing effects arising from surface delocalization of σ-electrons of the 3MR (48 kcal/mol for **1**). Both ring strain and surface delocalization increase in the series **1**, **2**, **3** with a slight dominance of the former effect. The chemical relevance of theoretical results is discussed with regard to the ability of 3MRs to interact with π-systems and to undergo addition reactions with electrophiles and nucleophiles. The observed regioselectivity in ring-opening reactions of oxiranes is explained.

I. Introduction

The peculiar properties of three-membered rings (3MR), in particular their ability to interact with π-systems and to stabilize carbenium ions, have intrigued experimentalists and theoreticians for many decades as is amply documented in the literature.[1] In order to rationalize experimental observations on 3MRs, the bonding of cyclopropane (**1**) has been interrelated with that of ethylene, on both the basis of the bent bond description advocated by Coulson and Moffit[2] and the Walsh model of **1**.[3] The bent bond model is often used to analyze energetics (strain)[4] and electron density distribution of 3MRs[5] while the Walsh model is more convenient for analyzing electronic interactions of 3MRs with attached substituents or an annelated ring system.[6] In principle, there is, however, no difference between the two models. They just provide complementary pictures of 3MRs with two different sets of basis orbitals, which are related by a unitary transformation.[7] Taking this into account, it should be possible

(1) (a) Charton, M. "Olefinic Properties of Cyclopropanes" In "The Chemistry of Alkenes"; Zabicky, J., Ed.; Wiley-Interscience: New York, 1970; Vol. 2. (b) Meijere, A. de, *Angew. Chem.* **1979**, *91*, 867-884; *Angew. Chem., Int. Ed. Engl.* **1979**, *18*, 809-826. (c) Gleiter, R. *Top. Curr. Chem.* **1979**, *86*, 197-285. (d) Lathan, W. A.; Random, L.; Hariharan, P. C.; Hehre, W. J.; Pople, J. A. *Top. Curr. Chem.* **1973**, *40*, 1-45. (e) Newton, M. D. In "Modern Theoretical Chemistry"; Schaefer, H. F., Ed.; Plenum Press: New York, 1977; Vol. 4, pp 223-275.

(2) Coulson, C. A.; Moffitt, W. E. *Philos. Mag.* **1949**, *40*, 1-35.

(3) Walsh, A. D. *Trans. Faraday Soc.* **1949**, *45*, 179-190.

(4) (a) Wendisch, D. In "Methoden der Organischen Chemie"; Houben-Weyl-Müller, E.; Thieme Verlag: Stuttgart, 1971; Vol. IV, 3, pp 17-27. (b) Liebman, J. F.; Greenberg, A. *Chem. Rev.* **1976**, *76*, 311-365.

(5) (a) Fritchie, C. J., Jr. *Acta Crystallogr.* **1966**, *20*, 27-36. (b) Hartman, A.; Hirshfeld, F. L. *Acta Crystallogr.* **1966**, *20*, 80-82. (c) Ito, T.; Sakurai, T. *Acta Crystallogr., Sect. B* **1973**, *B29*, 1594-1603. (d) Matthews, D. A.; Stucky, G. D. *J. Am. Chem. Soc.* **1971**, *93*, 5954-5959.

(6) (a) Hoffmann, R. *Tetrahedron Lett.* **1970**, 2907-2909. (b) Günther, H. *Tetrahedron Lett.* **1970**, 5173-5176. (c) Hoffmann, R.; Stohrer, W.-D. *J. Am. Chem. Soc.* **1971**, *93*, 6941-6948. (d) Jorgensen, W. L. *J. Am. Chem. Soc.* **1975**, *97*, 3082-3090.

(7) As has recently been shown, this is not longer valid considering only the bonding basis orbitals: Honegger, E.; Heilbronner E.; Schmelzer, A. *Nouv. J. Chim.* **1982**, *6*, 519-526.

0002-7863/85/1507-3800$01.50/0